Rethinking Charge trapping and detrapping dynamic without the sheet-charge approximation

Kin P. Cheung, Jason P. Campbell and Dmitry Veksler
National Institute of Standards & Technology, Gaithersburg, MD USA, kin.cheung@nist.gov

Charge-trapping/detrapping are common occurrences that affect MOSFET performance and reliability. To understand a broad range of MOSFET phenomena, we need to think through the dynamics of charge-trapping/detrapping. The standard approach to treat oxide trapped charge is to think of them as a thin sheet of uniform charge at the centroid location [1]. The effect of this sheet charge approximation is a uniform band-bending within the oxide as well as in the semiconductor near the interface. This picture completely dominates all discussions of charge-trapping in the literature.

In the struggle to understand random telegraph noise (RTN) magnitude, the notion that the trapped charge creates a localized region of reduced (sometimes to zero) inversion charge density has gained much attention [2-8]. Physically, it makes perfect sense that the trapped charge's strong electric field greatly changes the electrostatics in its immediate surrounding. While the RTN experiments are carried out in inversion, once an electron is trapped (assuming nFET), the strong electric field changes the local electrostatic to strong accumulation (hence the absence of inversion charges). With this in mind, when treating charge emission (detrapping) one can no longer assume that it is under inversion condition as in all published work so far. Instead, it should be under strong accumulation, leading to a very different process. In this paper, we explore what this means and how to reconcile experimental observations using RTN as an example.

One way to think of the local field due to a trapped charge is to think of the peaky potential surface resulting from the atomistic random dopant simulations [9] as shown in fig.1. For nFET, the ionized dopants are negatively charged. A trapped electron in the oxide should have similar peaky potential distribution except that the trapped charges tend to be near the interface so the peak is stronger than most dopant ions.

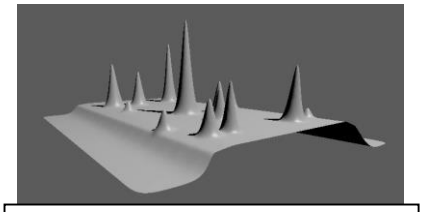

Fig. 1 Peaky surface potential in the MOSFET channel due to random dopant and electron trapped in oxide.

The peaky potentials puncture holes in the inversion layer. Within the hole, the electrostatics are very different. Fig. 2 illustrates the spatial transition from outside the trapped charge region, which is in inversion, to the center of the trapped charge region, which is in strong accumulation.

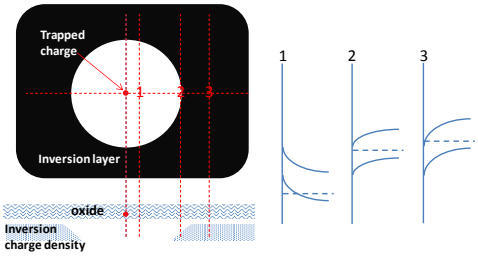

Fig. 2 A cored-out hole in the inversion layer surrounds the trapped electron. Three regions are identified to show the corresponding band bending at the bottom of the figure.

Fig. 3 illustrates the difference in band diagrams between the conventional sheet charge model and the localized charge model. A trap site inside the oxide captures a charge from inversion layer through tunneling (right hand side). Upon charge capture the trap energy reduces through multi-phonon relaxation [10]. Two sets of experiments in the literature both suggest that this energy drop is ~1.5 eV [11, 12]. Thus the new trap energy is shown to be below the valence band edge. The top panel of left hand side is the usual sheet charge picture whereas the bottom panel of left hand side is the local charge picture. It should very obvious that the emission process of these two cases are very different.

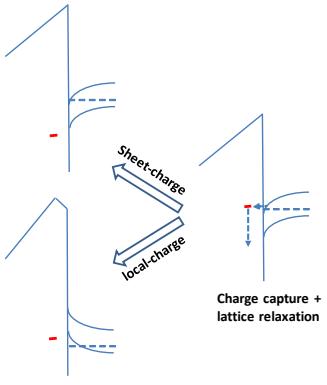

Fig. 3 Band diagram showing the capture of an electron by a defect site inside the oxide (RHS). The resulting band diagram for the conventional sheet charge model (top LHS) and the new local charge model (bottom LHS) are quite different.

We note that once multi-phonon relaxation is included, the emission kinetics are very difficult to explain using the conventional sheet charge model. The trapped charge must be thermally excited to overcome a large energy

barrier of ~ 1.5 eV. The probability is too low. Even if emission occurs to the gate electrode, there is still a large energy barrier. This is one of the reasons that RTN kinetics are difficult to model. Indeed, Kirton and Uren *et al.* are forced to conclude that the relaxation energy must be in the 20 to 150 meV range only [13]. Similarly, Palma *et al.* also relies on this same shallow relaxation to explain the RTN emission time constant [14]. These assumptions are, of course, not in agreement with experimental evidences [11, 12].

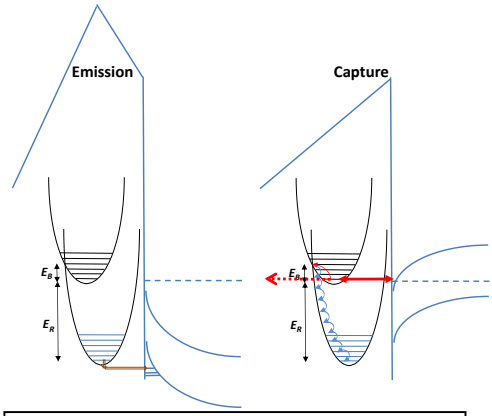

Fig. 4 Detailed charge capture and emission band diagram in the local charge model including multi-phonon relaxation.

With the local charge model, the opposite becomes true. The band diagram charge capture and emission in the local charge model is illustrated in more detail in fig.4. As can be seen, emission becomes very efficient. Capturing a hole from the accumulation layer is energetically extremely favorable. This would lead to very short emission time rendering RTN unobservable. This dilemma is resolved when we once again consider the highly localized nature of the field, leading to strong quantum confinement effect. This quantization is much stronger than the familiar inversion layer quantum confinement effect because the local accumulation layer is strongly confined in all three dimensions. Fig. 4 already shows the quantized energy levels in the accumulation layer.

Tunneling rate depends on two factors. One is the barrier (height and width), the other is the density of states (both the available carrier for tunneling and the available states to tunnel to). There are very few states in the accumulated region and that the first state is at least a fraction of an eV from the top of the conduction band. Note that the reduction in available states will cause the band bending to respond to the vertical field and become stronger, further reducing the density of states and increasing the distance of the first state from the top of the valence band. Thus even though the electron is at energy below the valence band edge, the emission still requires phonon assisted tunneling to reach the first state as illustrated in figure 4. Coupled with the low density of state available the emission rate is low enough for RTN to be observable in a reasonable measurement window.

The capture and emission process illustrated in figure 4 is consistent with the temperature effect on capture and emission time constants – both are thermally activated but with different activation energies [15].

Experimentally, the majority of the reported RTN time constants have the following behavior: as gate bias decreases, capture time constant increases and emission time constant decreases [15]. The model in figure 4 explains the gate bias dependent capture time constant easily, but what happen to the emission time constant? When gate overdrive reduces, quantum confinement also relaxes. The result is an increase in number of accessible states and a reduction in the energy offset of the first state from the valence band edge. Both effects will increase the emission rate and reduce the emission time constant – in agreement with majority of data in the literature.

[1] Wolters, D. R. and J. J. van der Schoot, *J. Appl. Phys*. **58**(2): 831-837(1985); See also Taur, Y. and T. H. Ning, *Fundamentals of Modern VLSI Devices,* page 87. Cambridge University Press, 1998. ISBN 0-521-55959-6. [2] L. D. Yau, and C.-T. Sah, *IEEE Trans. Electron Dev.*, **16**(2): 170-177(1969). [3] G. Reimbold, *IEEE Trans. Electron Dev.*, **31**(9): 1190-1198(1984). [4] A. Ohata, A. Toriumi, *et al., J. Appl. Phys.* **68**(1): 200-204(1990). [5] E. Simoen, B. Dierickx, *et al., IEEE Trans. Elect. Dev.,* **39**(2), 422(1992). [6] A. Asenov, R. Balasubramaniam, *et al., IEEE Trans. Elect. Dev.,* **50**(3): 839(2003). [7] K. Sonoda, K. Ishikawa, *et al., IEEE Trans. Elect. Dev.,* **54**(8): 1918(2007). [8] Southwick, R. G., K. P. Cheung, *et al., IEEE Silicon Nanoelectronics Workshop* (SNW), Kyoto, Japan, 2012. [9] A. Asenov *et al.*, *J. Comput. Electron*., **54**(8), 349-373(2009). [10] Henry, C. H. and D. V. Lang, *Physical Review B* **15**(2): 989 LP -1016(1977). [11] Lu, Y. and C. T. Sah, *J. Appl. Phys*. **78**(5), 3156-3159(1995). [12] Takagi, S., N. Yasuda, *et al., Int. Electron Devices Meeting*, (IEDM) 1996, pp323-326. [13] Kirton, M. J. and M. J. Uren, *Appl. Phys. Lett*. **48**(19), 1270-1272(1986). [14] Palma, A., A. Godoy, *et al. Phys. Rev. B* **56**(15), 9565-9574(1997). [15] Ralls, K. S., W. J. Skocpol, *et al, Phys. Rev. Lett.* **52**(3), 228 LP-231. (1984).